Paleomagnetism, structure and $^{40}Ar/^{39}Ar$ geochronology of the Cerro Mercado pluton, Coahuila: Implications for the timing of the Laramide orogeny in northern Mexico

Roberto S. Molina-Garza[1,*], Gabriel Chávez-Cabello[2], Alexander Iriondo[1,3], Mario Alberto Porras-Vázquez[2], and Guillermo Daniel Terrazas-Calderón[2]

[1] Centro de Geociencias, Universidad Nacional Autónoma de México,
Campus Juriquilla, Blvd. Juriquilla 3001, 76230 Querétaro, Qro., Mexico.
[2] Facultad de Ciencias de la Tierra, Universidad Nacional Autónoma de Nuevo León,
Carretera a Cerro Prieto Km. 8, 67700 Linares, Nuevo León, Mexico.
[3] Department of Geological Sciences, University of Colorado at Boulder,
Boulder, Colorado 80309, USA.
** rmolina@geociencias.unam.mx*

ABSTRACT

The Cerro Mercado pluton, emplaced in the Coahuila fold belt, contains magmatic, ductile, and brittle fabrics that suggest local and regional deformation during igneous emplacement, later affected by regional deformation in the area. The Cerro Mercado pluton intruded, deformed and uplifted Upper Cretaceous strata in the southern edge of the central depression of the Sabinas basin. A hornblende mineral separate from the pluton yielded a $^{40}Ar/^{39}Ar$ plateau age of 44.29 ± 0.19 Ma (1σ), interpreted as an approximation to the crystallization age of the monzonite. A younger biotite total fusion age of 41.23 ± 0.21 Ma (1σ) from a different rock sample is interpreted to represent slow cooling (~80°C/Ma) of the Cerro Mercado pluton. Paleomagnetic analyses of the pluton yield well defined remanent magnetizations of nearly uniform reverse polarity, with a grand mean of D=178.2° and I=-61.7° (N=9 acceptable sites; k=57.5, α95 = 6.8°). These data are discordant with respect to the Eocene reference direction, indicating apparent clockwise rotation (~8°) and inclination steepening (~21°). The simplest interpretation of the discordance is that northwestward tilting of the pluton occurred during basin inversion within a weakly right lateral transpressive regime with NNW directed contraction. The strain field is consistent with contraction during the Laramide orogeny. Also, remanence acquisition is contemporaneous with both tectonic and magmatic fabrics in the pluton indicating that it is syntectonic. This suggests – in agreement with stratigraphic data – that the Laramide orogeny in central Coahuila ended some time after about 44 Ma. We propose that reactivation of the San Marcos fault and other basement faults in the Sabinas basin represents the last manifestation of shortening produced by the Laramide orogeny. This was a short episode of deformation that ended by the time of emplacement of younger plutons of the Candela-Monclova magmatic belt ca. 41 Ma. This indicates that culmination of the Laramide orogeny in central Coahuila is only slightly younger than in central Chihuahua.

Keywords: Paleomagnetism, Laramide orogeny, Eocene, Sierra Madre Oriental, Coahuila, Mexico.

RESUMEN

El plutón Cerro Mercado, emplazado en el Cinturón plegado de Coahuila, contiene fábricas magmáticas dúctiles y frágiles que sugieren esfuerzos regionales y locales impuestos durante el emplazamiento, seguidos por deformación regional en el área. El plutón Cerro Mercado intrusionó, deformó y causó el levantamiento de estratos del Cretácico Superior en la margen sur de la depresión

central de la cuenca de Sabinas. Un separado de hornblenda del plutón arroja una edad de meseta de $^{40}Ar/^{39}Ar$ de 44.29 ± 0.19 Ma (1σ), que interpretamos como una aproximación a la edad de cristalización del plutón de monzonita. Un fechamiento de biotita de una segunda muestra del plutón arroja una edad más joven de 41.23 ± 0.21 Ma (1σ) que interpretamos como una edad de enfriamiento que, combinándola con la edad de hornblenda, permitiría calcular una tasa de enfriamiento relativamente lenta (~80°C/Ma) para el cuerpo plutónico de Cerro Mercado. Un estudio paleomagnético del intrusivo indica que en él existe una magnetización estable de polaridad casi uniformemente reversa, con una media de D=178.2° e I=-61.7° (N=9 sitios seleccionados; k=56.5, α_{95}=6.89°). Estos datos son discordantes con respecto a la dirección de referencia esperada para el Eoceno, indicando una rotación horaria (~8°) e inclinación más alta de la esperada (~21°). La interpretación más simple de estos datos es atribuir la discordancia a basculamiento hacia el noroeste durante inversión de la cuenca con una componente pequeña transpresiva lateral derecha con compresión dirigida hacia el NNW. Este campo de esfuerzos es consistente con contracción durante la orogenia Larámide. Además, la adquisición de la magnetización remanente es contemporánea con ambas fábricas magmática y tectónica, indicando que el plutón es sintectónico. Esto a su vez sugiere – de acuerdo con los datos estratigráficos – que la orogenia Larámide en Coahuila terminó después de hace 44 Ma. Proponemos que la reactivación de la falla de San Marcos y otras fallas de basamento en la cuenca de Sabinas representa la última manifestación del acortamiento producido por la orogenia Larámide. Este fue un episodio corto de deformación que terminó para el tiempo de emplazamiento de plutones más jóvenes del cinturón Candela Monclova ca. 41 Ma. Esto indica que la culminación de la orogenia Larámide en Coahuila central es solamente un poco más joven de lo propuesto para Chihuahua central.

Palabras clave: paleomagnetismo, Orogenia Larámide, Eoceno, Sierra Madre Oriental, Coahuila, México.

INTRODUCTION

The Laramide orogeny in northern Mexico and southwest Texas has been attributed to northeastward migration of stresses transferred from accretion of a volcanic arc in the Pacific through closure of a marginal basin and progressive shallowing of the Farallon slab in the Late Cretaceous and Early Cenozoic (James and Henry, 1991; Henry *et al.*, 1991; Goldhammer, 1999; Bird, 2002; Gilmer *et al.*, 2003; Chávez-Cabello, 2005). The end of this event can be dated stratigraphically, and is determined by the age of the oldest stratigraphic unit not affected by contractional deformation; or it can be dated using syntectonic and post-tectonic plutons that are contemporaneous with or postdate structures ascribed to the contractional event.

At Mariscal Mountain anticline, in the Big Bend National Park area of west Texas (Figure 1, inset), Laramide folding ended prior to intrusion of 37 Ma gabbro sills (Harlan *et al.*, 1995). In Chihuahua, termination of the Laramide orogeny is dated stratigraphically at about 44 Ma (the age of the Nopal Formation at Sierra Peña Blanca; Figure 1, inset; Reyes-Cortez and Goodell, 2000) or at about 46 Ma (the Ar-Ar age of a sill intruding a sequence of tilted gravels correlated with the Ahuichila Formation in eastern Chihuahua, east of Chihuahua city (Aranda-Gómez *et al.*, 2001). Biostratigraphic studies at La Popa basin (Figure 1, inset) suggest that the Laramide orogeny in Coahuila had ended by late Eocene time (Vega-Vera and Perrillat, 1989). Iriondo *et al.* (2005) proposed that the Laramide orogeny in NW Sonora ended *ca.* 40 Ma, based on geochronology of greenschist facies ductile fabrics associated with compressional shear zones.

Paleomagnetic data for the Mariscal Mountain gabbro sills suggest that previous claims of vertical axis rotations in the Trans-Pecos region are equivocal (Harlan *et al.*, 1995). Previous paleomagnetic studies either yield statistically insignificant rotation estimates (*e.g.*, Sager *et al.*, 1992), or they fail to adequately average secular variation of the geomagnetic field (Harlan *et al.*, 1995). Statistically significant vertical-axis rotations have been proposed for Eocene volcanic rocks in central Chihuahua on the basis of paleomagnetic data (Urrutia-Fucugauchi, 1981). Paleomagnetic data suggesting vertical axis rotations in central Coahuila have been reported recently (González-Naranjo, 2006; Arvizu-Gutiérrez, 2006); they have been also observed within the Sierra Madre Oriental (SMO) fold and thrust belt in the city of Saltillo area (Nowicki *et al.*, 1993), in localities near the city of Torreón close to the SMO front in southern Coahuila (Kleist *et al.*, 1984), and in the Difunta Group in the Parras Basin (Nairn, 1976).

Here we present structural, geochronological, magnetic fabric, and paleomagnetic data for the Cerro Mercado pluton in central Coahuila, northeast Mexico. These data suggest that emplacement of this pluton, which forms part of the Candela-Monclova magmatic belt, is syntectonic with respect to the contractional Laramide orogeny. This interpretation is based on deformation at its margins, magmatic foliation and internal structure, the relationship of emplacement with respect to folding, magnetic fabric patterns, tilt of the pluton, and its age relative to synorogenic sedimentation. We also discuss the implications of this interpretation for the timing of the Laramide orogeny in northeast Mexico.

There is considerable debate on the relation of magmatic fabrics, emplacement, and deformation in plutonic

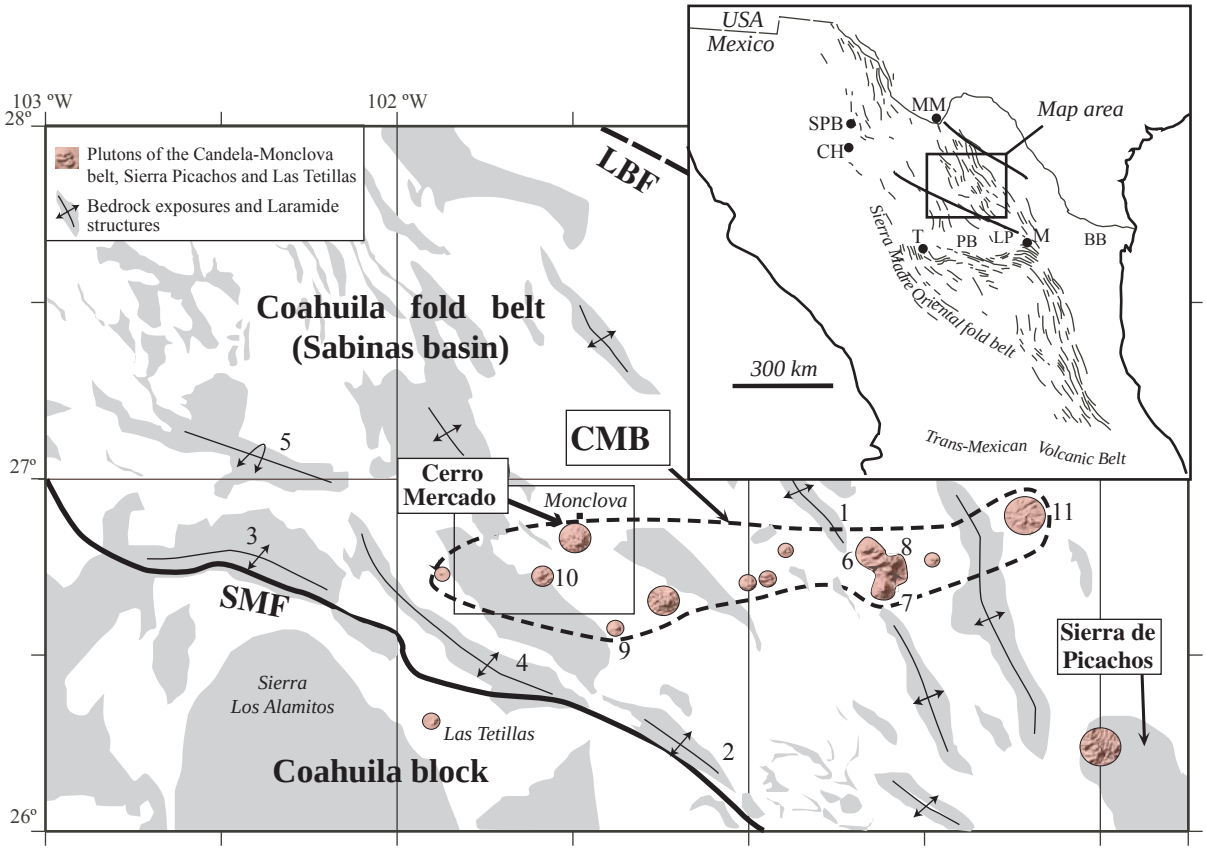

Figure 1. Regional map of central Coahuila state showing the principal exposures of bedrock, Laramide structures, and the trend of plutonic rocks of the Candela-Monclova belt. The inset shows the location of the map area and the general trend of the Sierra Madre Oriental fold belt. Localities mentioned in the text include: BB: Burgos basin; CH: Chihuahua city; LP: La Popa Basin; M: Monterrey city; MM: Mariscal Mountain anticline; PB: Parras basin; SPB: Sierra Peña Blanca; T: Torreón city. The box indicates the area of Figure 2 around Cerro Mercado. SMF: San Marcos fault; LBF: La Babia fault; CMB: Candela-Monclova magmatic belt. Other symbols: 1: Oballos anticline; 2: La Gavia anticline; 3: Sierra la Fragua; 4: San Marcos-Pinos anticline; 5: Sierra la Madera; 6: Cerro Boludo pluton; 7: Marcelinos pluton; 8: Carrizal pluton; 9: Providencia pluton; 10: La Soledad pluton; 11: La Iguana pluton.

rocks. But there are general features —not always diagnostic— typical of pretectonic, syntectonic, and post-tectonic plutons (Lamourux *et al.*, 1980; Oliver and Wall, 1987, Paterson and Tobisch, 1988; Paterson *et al.*, 1991; Brun and Pons, 1981; Hutton, 1981; Guineberteau *et al.*, 1987). Paleomagnetic and magnetic fabric data provide additional criteria for identifying syn-tectonic plutons (Pignotta and Benn, 1999). We submit that these data strengthen the interpretation of Cerro Mercado pluton as syntectonic.

REGIONAL GEOLOGY

Igneous rocks of Eocene-Oligocene age have restricted distribution in northeast Mexico. In Coahuila, these rocks include almost exclusively shallow hypabyssal bodies that intrude a deformed Upper Jurassic–Cretaceous marine sedimentary sequence. This igneous suite overlaps temporally rocks that form part of the alkaline province of northeast Mexico (Robin and Tournon, 1978; Aranda-Gómez *et al.*, 2005), as well as rocks of the Sierra Madre Occidental magmatic province, and rocks of the Trans-Pecos magmatic province of southwest Texas (James and Henry, 1991).

Paleogene plutonic rocks in Coahuila are included in the intrusive suite of the Candela-Monclova magmatic belt (CMB, Sewell, 1968). The belt consists of at least 16 intrusions that define an east-west oriented band nearly 200 km long, cutting across the NW-SE trending Laramide structural grain of the Coahuila fold belt between 26.5°–27° N and 100°–102° W (Figure 1). The dominant rock types in the CMB are monzonites, monzodiorites, and quartz monzonites (Morton-Bermea, 1995; Chávez-Cabello, 2005). It has been proposed that these intrusions were emplaced along the limits of basement highs south of the Sabinas basin, a paleogeographic element in central Coahuila (Chávez-Cabello, 2005).

According to Sewell (1968) the age of the intrusions of the CMB ranges between 43 and 35 Ma (recalculated K-Ar dates). Geochemically, the CMB intrusions include two magmatic series: a high-K calc-alkaline series and a shoshonitic series (Morton-Bermea, 1995; Cano-González, 2002; Tovar-Cortés, 2002; Chávez-Cabello, 2005). Previous studies suggested that magmas were produced by subduction

of the Farallon plate (Chávez-Cabello, 2005; and references therein). The great majority of the intrusions are subvolcanic bodies with porphyritic textures, but there are exceptions such as Cerro Mercado.

The Coahuila fold belt developed in the Mesozoic marine sedimentary sequence of the Sabinas basin. It is limited to the southwest by the Coahuila block (Figure 1), along the San Marcos fault (Charleston, 1981; Padilla y Sánchez, 1982; McKee *et al.*, 1990; Eguiluz de Antuñano, 2001; Chávez-Cabello *et al.*, 2005). To the northeast it is limited by the Burro-Peyotes platform along the La Babia fault (Charleston, 1981) or by the Boquillas del Carmen–Sabinas lineament (Padilla y Sánchez, 1982). The sedimentary sequence of the Sabinas basin was folded and thrusted over the Coahuila block, and to a lesser degree over the Burro-Peyotes high, during the Laramide orogeny (Padilla y Sánchez, 1982; McKee *et al.*, 1990). Recently, Chávez-Cabello *et al.* (2005) have shown that following an episode of northeast-directed Laramide thrusting, the San Marcos fault was reactivated as a reverse fault. Reactivation of basement faults generated drape folds with southwest-directed tectonic transport attributed to a late phase of the Laramide orogeny. The CMB intrusions were emplaced between NW-SE trending folds along the western sector of the Coahuila fold belt and NNW-SSE folds along its eastern sector. Not all of the intrusions, however, show cross-cutting relations with Laramide fold structures as some occur as isolated laccoliths.

Chávez-Cabello (2005) suggested that the southern half of the Coahuila fold belt is a zone characterized by the coexistence of high-angle and low-angle reverse faults with associated asymmetric folds. Relatively thin evaporite deposits also characterize this area of the fold belt. Crystalline basement occurs at relatively shallow levels compared to other parts of the fold belt to the north. In the area along the La Fragua, La Madera and San Marcos–Pinos regional folds (Figure 1), folding and faulting are complex and appear to have occurred in two phases. The first phase is characterized by detachment along favorable stratigraphic levels with generation of fault-bend folds; during this phase, tectonic transport was northward. A second phase of deformation is characterized by reactivation of basement faults, with minor tectonic transport to the southwest. It is within this structurally complex zone that the great majority of the intrusions of the CMB were emplaced.

In contrast, the axis of the Sabinas basin to the north is characterized by isolated anticlines trending NW-SE to NNW-SSE that are separated by broad synclinal valleys. The traces of the folds are sigmoidal to slightly curved, and their cores are often intruded by Jurassic evaporites (*e.g.*, Oballos and La Virgen anticlines; Figure 1).

In addition to models that assume collision of a fringing arc in the Pacific, a flat slab subduction model has been also invoked to explain Laramide deformation in NE Mexico (Bunge and Grand, 2000; Bird, 2002; Chávez-Cabello, 2005). Plutons of the CMB have a chemical signatures typical of subduction-related magmas, and they lie ~900 km east of the paleo-trench along the Pacific margin (Morton-Bermea, 1995; Chávez-Cabello, 2005). The geochemistry and location of the plutons thus support the model of flat subduction in this region of the Cordillera.

GEOLOGY OF CERRO MERCADO

Cerro Mercado is located in the western sector of the CMB, just south of the city of Monclova. The intrusion crops out over a surface of about 12.8 km^2 at the southeastern end of Sierra Sacramento (Figure 2). This sierra is a complex structure formed by two anticlines that resemble a NW-SE

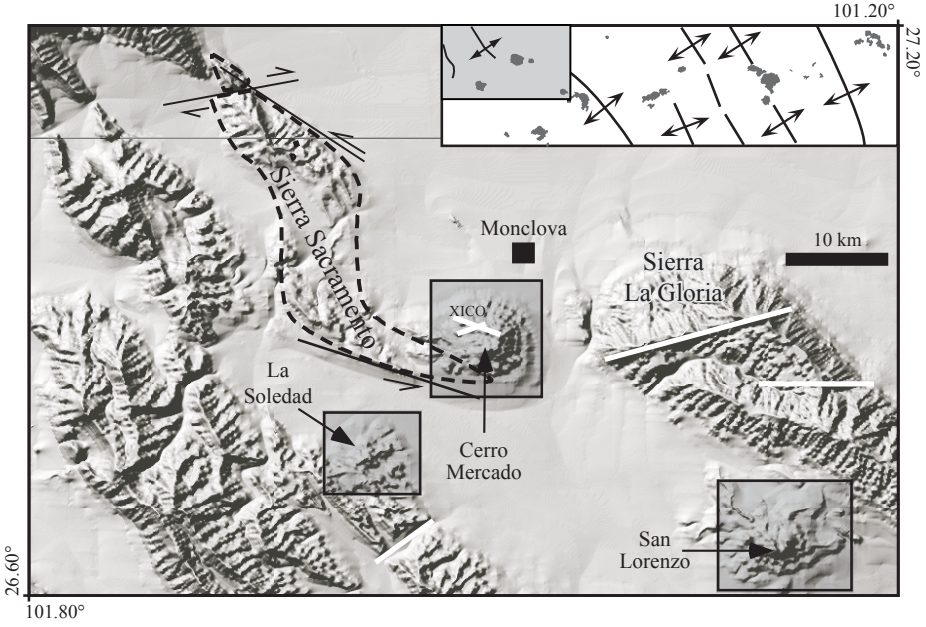

Figure 2. Digital elevation map of the area around Cerro Mercado showing the principal Laramide structures and the plutonic rocks that crop out in the area. The inset shows in a gray box the area of the digital elevation map, and its location with respect to the trend of the plutons of the Candela-Monclova belt (dark gray).

oriented sigmoid (Figure 2). At first glance, the relationship of the Cerro Mercado pluton to this structure may suggest post-tectonic emplacement, but structural relationships are equivocal. Emplacement caused domal uplift of the Cretaceous sequence (Figure 3), but domal uplift alone does not provide a compelling argument to establish temporal relationships between emplacement and regional deformation. Mapping at a scale 1:10,000 and structural observations (Figure 3; described below) show that the pluton has irregular borders, most notably along its northeastern margin.

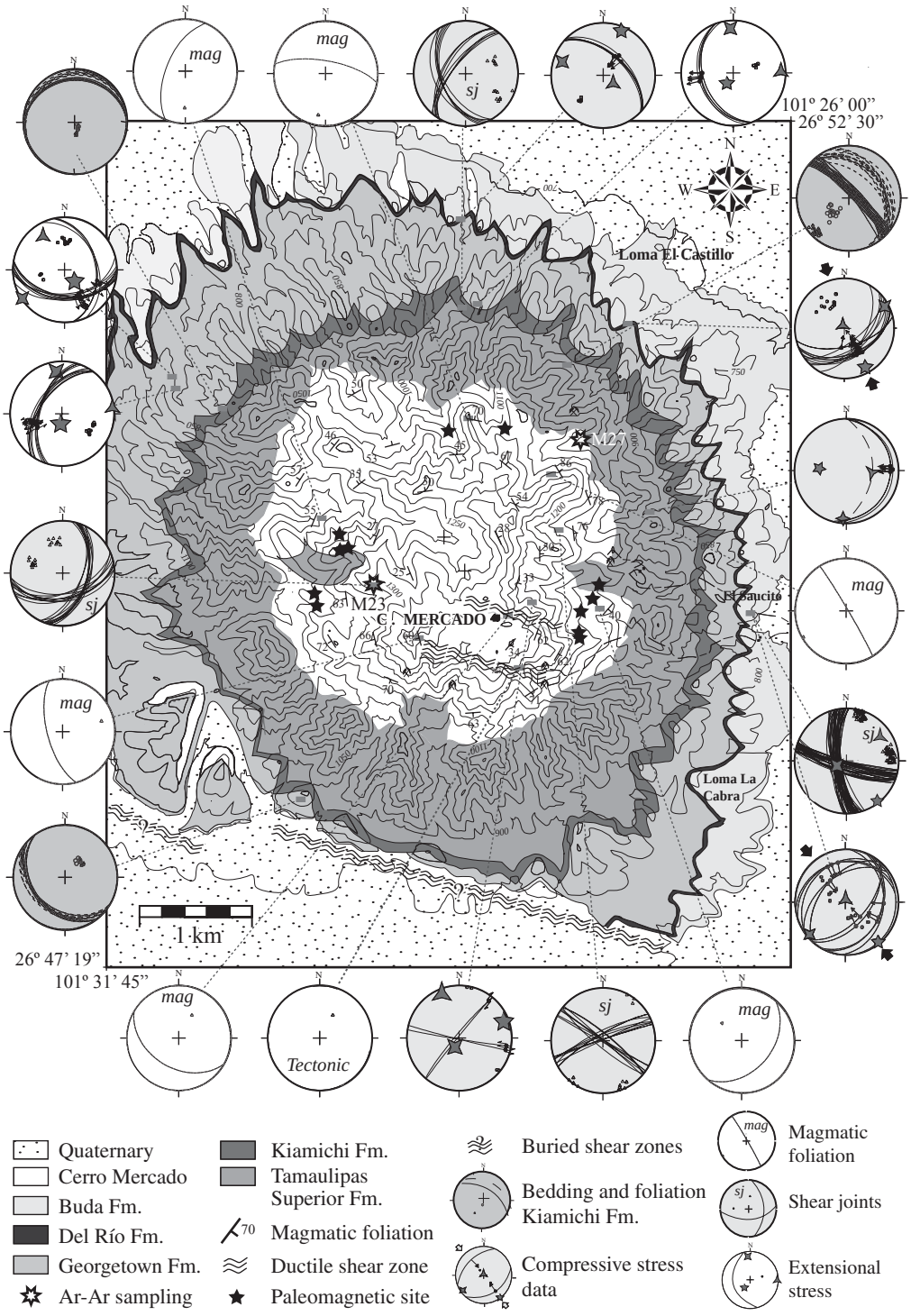

Figure 3. Geologic map of Cerro Mercado. The pluton shows irregular contacts with the host rock, some stopped blocks in the southwest area, and radial uplift of the Upper Cretaceous sequence. Intense deformation is present in the south internal zone of the pluton, represented by ductile shear zones. A zone of fragile deformation is present in the country rocks in the south. Both, the fragile and ductile zones are interpreted as coeval with pluton emplacement and regional contraction of the Laramide orogeny in Coahuila.

Country rocks are well exposed in the southwestern part of the pluton, where sills were emplaced along argillaceous horizons of the Kiamichi and Del Río Formations (Washita Group). The sills are apparently tilted, as they dip radially outward, suggesting late expansion of the pluton. Facies in the pluton vary from monzodiorite, to quartz monzonite, to monzonite, but not in a systematic way.

There is clear evidence of both magmatic and subsolid to solid-state foliations at Cerro Mercado. Magmatic foliation is defined by alignment of hornblende and biotite phenocrysts, and shows a generalized concentric fabric that parallels the pluton margins (Figure 3). Sub-solid to solid-state fabrics are present along shear zones with cataclastic to mylonitic textures, notably in the southern and southeastern sectors of the pluton (Figures 3 and 4). Although ductile fabrics depend also on strain rate, which may be high during pluton emplacement, these fabrics in a hypabyssal pluton must be syn-emplacement. Hypabyssal plutons are emplaced at shallow crustal levels where ambient conditions only allow crystal plastic deformation to operate if the temperature is high (above 300 °C for quartz, and below the solidus). Thus regional stress must have been responsible for generating ultramylonites in the shear zones at Cerro Mercado. The nearly WNW strike of the shear zones is notably discordant to magmatic foliation, and they are as much as 1.5 m thick. Both magmatic and subsolid to solid-state fabrics are interpreted to be the result of regional contraction imposed during emplacement. Given the regional setting, it is unlikely that ductile shear zones would be present in a post-tectonic hypabyssal pluton.

Localized solid-state foliation at Cerro Mercado is clearly parallel to the shear zones. This deformation in the pluton is manifest as mylonitic fabric oriented 276°/65°N, and is formed by quartz and K-feldspar porphyroclasts with geometries consistent with right-lateral sense of shear (Figure 4). In addition to this fabric, Cerro Mercado rocks display a well-developed set of conjugate fractures also consistent with the kinematics of faults within the shear zones. The domal structure of the pluton and its host rock clearly show that the pluton deformed the Cretaceous sequence radially by local expansion or ballooning (Sylvester *et al.*, 1978; Holder, 1979; Pitcher, 1979; Courrioux, 1987; Ramsay, 1989). Most deformation recorded by the host rock (fractures and faults) demonstrate this (Figure 3). However, the domal uplift interacted with regional structures. The clearest evidence of this interaction is the truncation of the Upper Cretaceous sequence (Washita Group), south of the intrusion, by a WNW striking shear zone, which is parallel to the termination of Sierra Sacramento to the east (Figures 2 and 3). These features are characteristic of syntectonic plutons. Cerro Mercado is thus syntectonic with respect to regional deformation. Two stations on the eastern side of the pluton record local NW shortening related to emplacement of a nearby subvolcanic body not mapped.

$^{40}Ar/^{39}Ar$ GEOCHRONOLOGY

Analytical methods for ^{40}Ar-^{39}Ar analyses are described in the appendix. Hornblende from monzonite sample M-23 shows a well-behaved age spectrum forming a plateau at 44.29 ± 0.19 Ma for 89.2% of the total $^{39}Ar_K$ gas released from the sample (Figure 5a). The K/Ca diagram indicates low and constant apparent element ratios indicating homogeneity/purity of the hornblende mineral separate. This plateau age is supported, within limits of analytical precision (1σ), by the less precise inverse correlation age of 43.52 ± 0.65 Ma (Figure 5c). The plateau age of 44.29 ± 0.19 Ma is interpreted as the time when the monzonite intrusive (sample M-23) cooled below ~530 ± 40°C, the closure temperature of hornblende (Harrison, 1981; McDougall and Harrison, 1999). Therefore, this plateau age represents a minimum possible age (cooling age) for the pluton but represents our best estimation for the age of crystallization of the Cerro

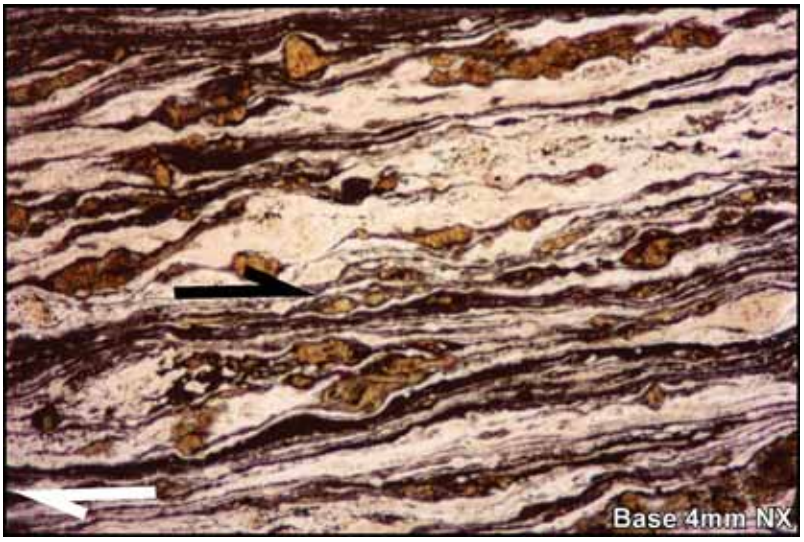

Figure 4. Photomicrograph of mylonite from the WNW shear zone in the south-central part of Cerro Mercado. The original rock is a quartz-monzonite. The photograph shows white bands of quartz, dark hornblende and biotite, and large broken crystals of feldspar.

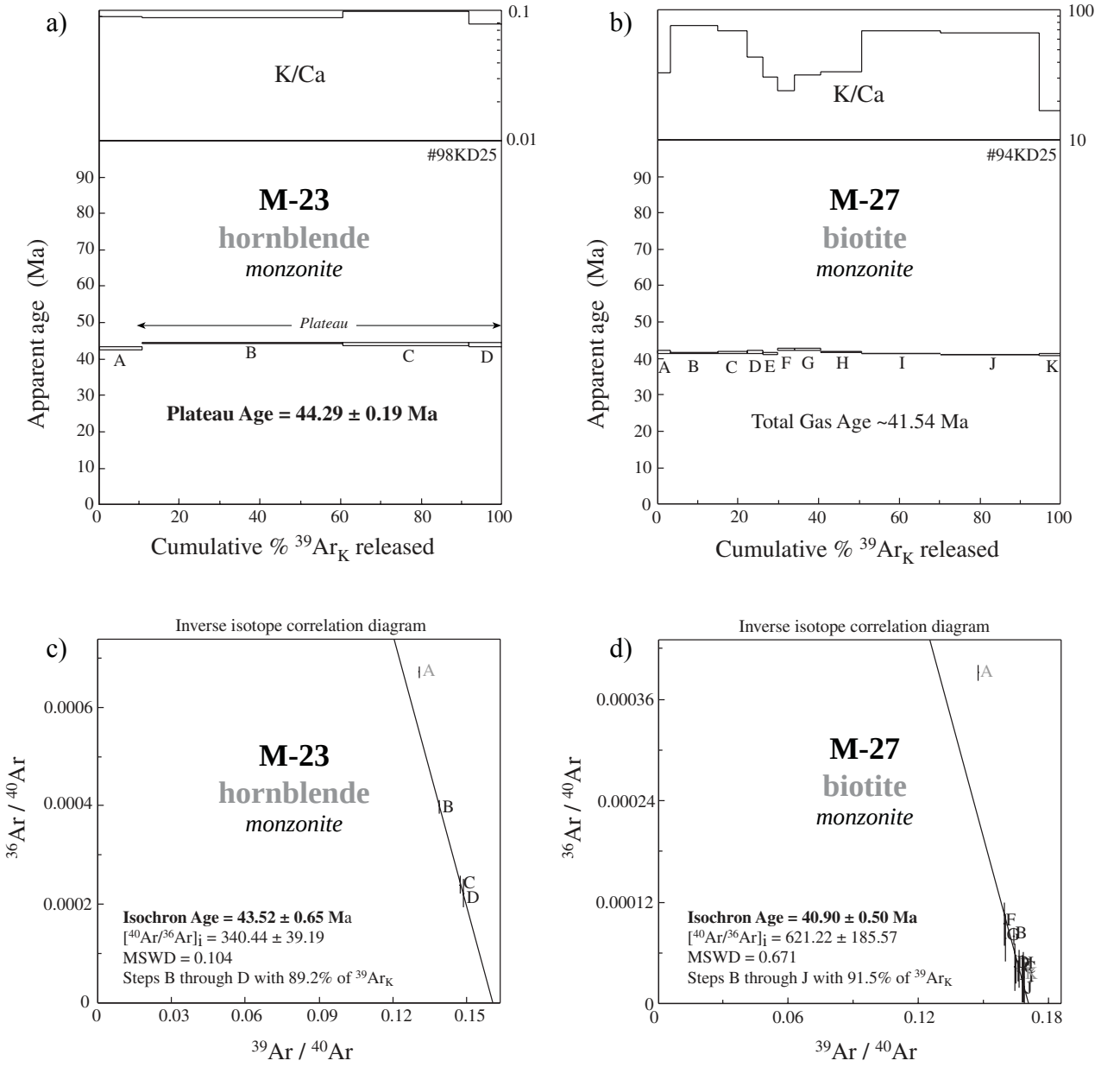

Figure 5. $^{40}Ar/^{39}Ar$ step-heating data for the Cerro Mercado monzonite. a-b: Age spectrum and K/Ca diagrams for hornblende and biotite mineral separates from monzonite samples M-23 and M-27. c-d: Inverse-isotope correlation diagrams for the same mineral separates showing the calculated isochron ages and their statistical constraints (at 1σ level of precision).

Mercado monzonite.

The biotite age spectrum for sample M-27 (#94KD25) is relatively concordant but does not define a plateau as defined above (Figure 5b). We have determined an isochron age at 40.90 ± 0.50 Ma, which, within limits of analytical precision (1σ), supports the more precise total fusion age at 41.23 ± 0.21 Ma (Table 1). The presence of small amounts of chlorite in this biotite sample could be inferred by the older hump (small convex upward) in the age spectrum between steps E-H (Figure 5b). In our data, we also observe a decrease in the K/Ca ratios for the same heating steps. This effect is most likely due to $^{39}Ar_K$ recoil caused by the low retentivity of chlorite. The result of loss of $^{39}Ar_K$ from our biotite grains is an anomalous increase in the $^{40}Ar/^{39}Ar$ and an increase in the apparent age for those temperature steps. Effects of intergrown chlorite in biotite for $^{40}Ar/^{39}Ar$ degassing experiments, and interpretation of spectra, are carefully discussed in Hess *et al.* (1987). In conclusion, the biotite total fusion age at 41.23 ± 0.21 Ma is interpreted as the time when the monzonite intrusive (sample M-27) cooled below ~280 ± 40 °C, the closure temperature of biotite (Harrison *et al.*, 1985).

The age difference between hornblende and biotite (~3 Myr) suggests the Cerro Mercado monzonite intrusive

Table 1. $^{40}Ar/^{39}Ar$ step-heating data for monzonite rocks from Cerro Mercado, Candela-Monclova magmatic belt (CMB).

Step	Temp. (°C)	%^{39}Ar of total	Radiogenic yield (%)	$^{39}Ar_k$ (moles x 10^{-12})	$^{40}Ar^*/^{39}Ar_k$	Apparent K/Ca	Apparent K/Cl	Apparent age (Ma)	Error (Ma)
***M-23**; Monzonite; hornblende;* J = 0.003921 ± 0.35%; wt. = 94.2 mg; #98KD25; coord: 101°29'44"W—26°49'24"N									
A	1100	10.8	80.2	0.103128	6.142	0.090	8.0	42.93	± 0.20
B	1200	49.9	88.2	0.476092	6.355	0.090	8.0	44.40	± 0.10
C	1250	31.3	92.9	0.298529	6.308	0.100	9.0	44.08	± 0.17
D	1300	8.1	93.4	0.076991	6.277	0.080	8.0	43.86	± 0.30
Total Gas		100.0	89.2	0.954740	6.311	0.091	8.5	44.10	
89.2% of gas on plateau in steps B through D							**Plateau age =**	**44.29**	**± 0.19**
***M-27**; Monzonite; biotite;* J = 0.003918 ± 0.35%; wt. = 22.8 mg; #94KD25; coord: 101°27'49"W—26°51'21"N									
A	750	3.1	88.4	0.079176	5.982	33.04	87	41.79	± 0.16
B	850	11.9	97.6	0.303778	5.949	76.11	97	41.56	± 0.05
C	900	7.2	98.9	0.183308	5.960	69.69	97	41.64	± 0.09
D	950	4.1	98.8	0.103966	5.981	43.65	95	41.79	± 0.16
E	1000	3.4	98.8	0.087171	5.928	30.45	95	41.42	± 0.19
F	1050	4.2	97.2	0.105953	6.089	23.77	92	42.53	± 0.18
G	1100	6.7	97.7	0.171468	6.096	31.88	95	42.58	± 0.14
H	1150	10.2	98.7	0.259870	5.999	33.82	98	41.91	± 0.06
I	1200	19.5	99.1	0.498232	5.907	68.89	77	41.27	± 0.02
J	1250	24.3	99.6	0.621039	5.886	67.35	100	41.13	± 0.03
K	1350	5.4	99.1	0.137381	5.886	16.98	99	41.13	± 0.14
Total Gas		100.0	98.5	2.551342	5.945	55.25	93	41.54	
***M-27**; Monzonite; biotite total fusion;* J = 0.003917 ± 0.35%; wt. = 5.0 mg; #95KD25; coord: 101°27'49"W—26°51'21"N									
A	1450	100.0	97	0.499257	5.902	41.24	64	41.23	± 0.21

Ages calculated assuming an initial $^{40}Ar/^{36}Ar$ = 295.5± 0.; All precision estimates are at the one sigma level of precision;. Ages of individual steps do not include error in the irradiation parameter J. No error is calculated for the total gas age.

cooled relatively slowly, which is consistent with the relatively coarse texture of the pluton. The ~250 °C closure temperature difference between hornblende and biotite (see above), and their age difference, could be used to estimate a cooling rate of ~80 °C/Ma for the Cerro Mercado pluton. If one were to extrapolate this cooling rate, actual crystallization may have occurred two to three million years earlier. But without U-Pb data, and without a good estimate of the geothermal gradient during cooling, this extrapolation is uncertain. Furthermore, the cooling rate was estimated from rocks from different localities within the Cerro Mercado pluton (Figure 3).

PALEOMAGNETISM

Sampling and methods

Paleomagnetic data for Cerro Mercado are based on stepwise demagnetization of samples from 11 sites collected throughout the pluton (Figure 3); one additional site was collected in limestone of the host rock. Each paleomagnetic site consists of five to seven individually oriented samples collected within an area of several square meters. The samples were oriented with magnetic and solar compasses, which yielded no systematic differences between orientations.

The samples were subjected to progressive alternating field (AF) and thermal demagnetization using commercial equipment. A JR-5 spinner magnetometer housed in a magnetically shielded room, at the Centro de Geociencias (UNAM) Paleomagnetic Laboratory, was used for remanence measurements. A small set of pilot samples were measured using a 2G Enterprises cryogenic magnetometer at the University of New Mexico. Magnetic anisotropy measurements were obtained using a KLY-3 Kappabridge. The vectorial composition of the remanence was determined from inspection of orthogonal demagnetization diagrams (Zijderveld, 1967), and the direction was determined using principal component analysis (PCA) (Kirschvink, 1980). When demagnetization results did not isolate the characteristic magnetization, great circles and stable end points were combined in order to calculate the site means by using the algorithms of Bailey and Halls (1984) and McFadden and McElhinny (1988), but site means were better defined by the first method and those results are reported. For the overall mean, we assumed that the site mean distribution is reasonably described by a Fisher distribution (Fisher, 1953).

Demagnetization results

Samples collected at Cerro Mercado have a relatively complex magnetic record as their behavior is multicomponent, but separation of magnetic components is relatively

straightforward. The natural remanence is of relatively high intensity (tens to hundreds of mA/m), except in the limestones of the host rock, where it is less than 0.5 mA/m. Most samples respond well to AF demagnetization, removing first a north directed magnetization of moderately steep positive inclination and low coercivity (generally less 16 mT), to reveal a characteristic magnetization (ChRM) of reverse polarity (south directed and steep negative; Figure 6a). The ChRM is of high coercivity, being removed with inductions of 40 to over 120 mT. Decay of the ChRM is somewhat noisy, perhaps because of acquisition of small anhysteretic remanences during the demagnetization experiments. Nonetheless, line fits anchored to the origin using PCA yield acceptable mean angular deviation (MAD) values generally <10°. Repeated treatment with liquid nitrogen (Dunlop *et al.*, 1997), removes spurious magnetizations of high intensity and variable direction, which are also of very low coercivity (below 10 mT). For this, samples were immersed in liquid nitrogen for 5 minutes, then measured and immersed again in up to five cycles labeled N1 to N5 in demagnetization diagrams (Figures 6c and 6d). The overprint is thus often a composite magnetization that forms curved demagnetization trajectories. In the samples illustrated in Figures 6c and 6d there are three components of magnetization. The spurious magnetizations are interpreted as isothermal remanent magnetizations induced by lightning and the north directed magnetizations are interpreted as viscous magnetizations of Brunhes age. The nitrogen treatment does not completely remove the north directed overprint (Figure 6c), but the combination of liquid nitrogen, AF, and thermal demagnetization often produces results of excellent quality that isolate the ChRM (Figure 6d).

In many cases, demagnetization trajectories define great circles tracking towards the south and to the upper hemisphere, but alternating fields of up to 130 mT are not sufficient to completely remove the north directed magnetization and isolate the component of reverse polarity (Figure 6b), or demagnetization trajectories become erratic at high fields. For samples where the reverse polarity magnetizations is not completely isolated, we calculated great circle trajectories which are well defined as illustrated in the stereographic projection of Figure 6b; only samples with MAD

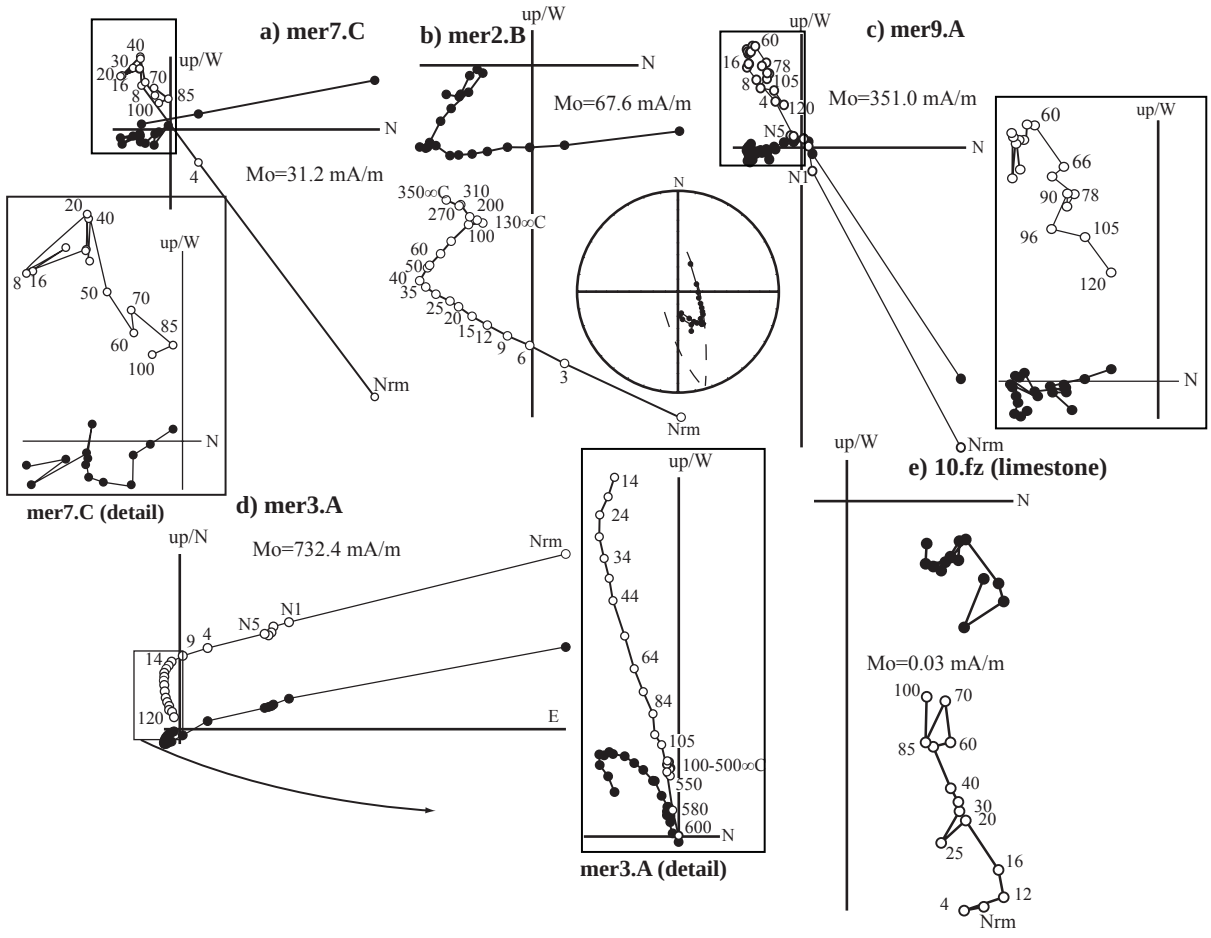

Figure 6. Orthogonal demagnetization diagrams (Zijderveld, 1967) of selected samples of the Cerro Mercado pluton (a-e) and its country rock (f). Solid (open) symbols are projections on the horizontal (vertical) plane. Detail of the demagnetization trajectory near the origin is included for a, c and d. Mo is the initial NRM.

values smaller than 14° were used in final calculations.

In most cases AF treatment removes the ChRM, suggesting that the remanence resides in a cubic phase such as magnetite or titanomagnetite. Maximum coercivities exceed 120 mT (Figure 6c), but maximum unblocking temperatures do not exceed 600°C (Figure 6d, detail). We also note that thermal treatment after 130 mT continues removal of a north directed and positive inclination magnetization (Figure 6b). Thus hematite may also carry part of the overprint.

Isothermal remanent acquisition curves (IRM) nearly reach saturation with inductions of 0.3 T (Figure 7). This confirms that a cubic phase is the dominant magnetic mineral. But a small increase in remanence between 0.3 and 1.5 T is attributed to hematite. Thin section inspection of the samples shows that thin oxidation rims are present on some of the magnetite grains. The high unblocking temperatures are more consistent with low-Ti magnetite as the main remanence carrier. Liquid nitrogen demagnetization indicates the presence of multi-domain (MD) magnetite grains. These results suggest that the magnetic mineralogy consists of large MD magnetite grains, small PSD or SD low-Ti magnetite grains of high coercivity, and a small fraction of hematite of secondary origin.

In the great majority of the sites the ChRM is of reverse polarity. Site 10, collected in the host rock (recrystallized limestones of the Tamaulipas Superior Formation), is of normal polarity and site 9, adjacent to the contact but within the intrusion, contains samples of both normal and reverse polarity. The magnetization in the limestone is rather weak, only one sample produced a linear trajectory to the origin (north-northeast directed and steep positive; Figure 6e), the rest yield large MAD values and were thus rejected. The hypothesis that the antipodal of that sample was drawn from the same population as the rest of the pluton directions cannot be rejected with a 95% confidence. This, in combination with the presence of both polarities in the site in the pluton closest to the contact, suggests that the recrystallized limestone was heated by the intrusion and acquired a TRM. The near uniform reverse polarities are consistent with remanence acquisition and closure of the Ar-Ar system in hornblende (530 ± 40°C) during chron C20r (43.8–46.2 Ma; Cande and Kent, 1995), in the early middle Eocene.

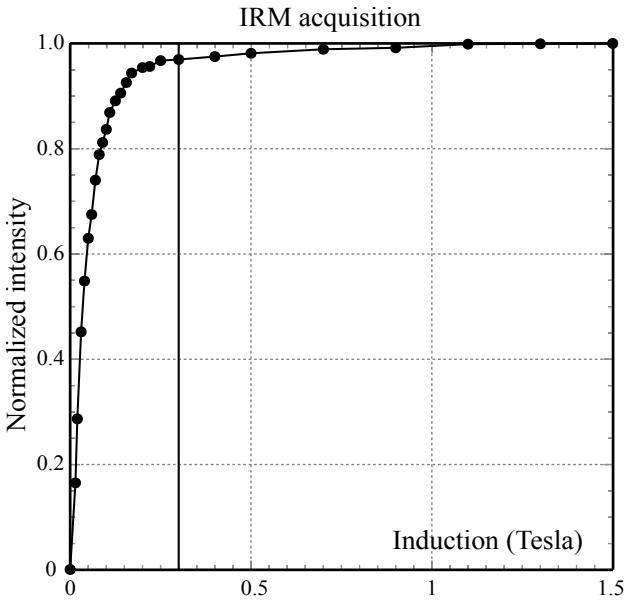

Figure 7. Isothermal remanent (IRM) acquisition curve showing the typical behavior observed in samples from Cerro Mercado. Notice near saturation with inductions of 0.3 T.

Site means calculated from sample directions and great circle trajectories (Figure 8) are reasonably well defined, with k values greater than 30 and $\alpha_{95}<15°$. Sites with $\alpha_{95}>15°$ were excluded from the overall mean. Confidence intervals are relatively large at most sites because means are defined by only four or five samples. The grand mean, based on 9 sites, is of D=178.2° and I=-61.7° (k=57.5, α_{95}=6.8°). Between-site dispersion is low, with an estimated angular standard deviation of 10.8°, consistent with averaging paleosecular variation at this low latitude (McFadden and McElhinny, 1984). We also believe that slow cooling of the pluton may have contributed to partially average secular variation.

The grand mean is discordant with respect to the expected Eocene direction of North America (Figure 8), which for the study area is of D=170.2° and I=-40.7°. This direction was calculated from a reference pole at 80.5°N–149.4°E, for the interval 30–40 Ma after Diehl *et al.* (1988). The observed direction is discordant in declination and inclination; rotation and flattening values (R and F) are estimated at 8.0°±15.6° and 21.0°±6.9°, respectively (errors calculated after Demarest, 1983). The result is not significantly different if we use a different reference pole, such as Symons *et al.* (2003).

The issue as to whether or not demagnetization results successfully isolate a characteristic magnetization may contribute to errors in the interpretation of paleomagnetic data. For the samples of Cerro Mercado, the ChRM is of nearly uniform reverse polarity, and the overprint is of positive inclination. We thus lack the means to perform a reversal test. Nonetheless, a partial contamination of the ChRM by unremoved overprinting components would shallow the average inclination. The inclination observed is steeper than expected; therefore, incomplete removal of an overprint cannot explain the discordance.

MAGNETIC FABRIC

Anisotropy of magnetic susceptibility (AMS) is well defined at most sampled sites (Figure 9), but a clear exception is site 2 represented by a small number of samples. The fabric is predominantly oblate, ranging from weakly oblate to strongly oblate. Despite the small number of samples per site, all susceptibility axes are well clustered,

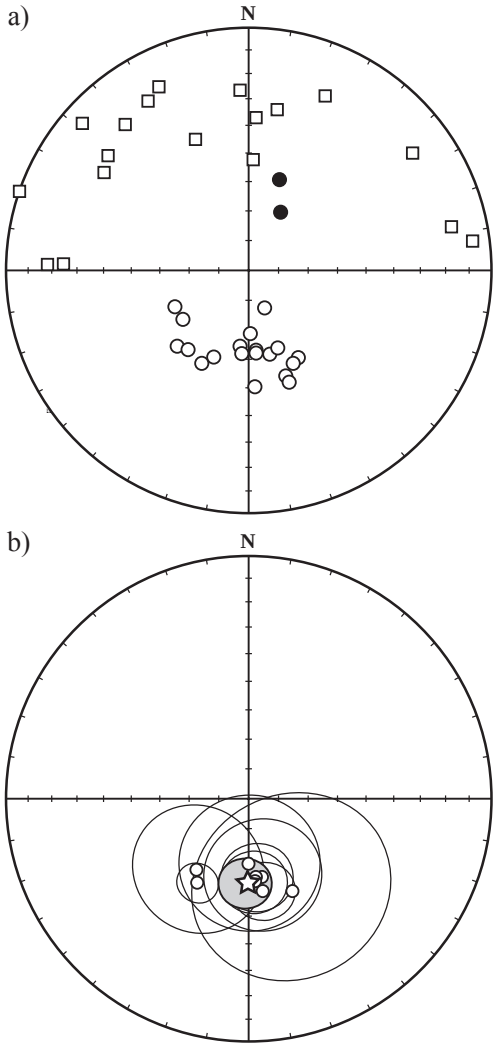

Figure 8. Stereographic projections of sample directions (a), and site means with confidence intervals (b) for the Cerro Mercado pluton. Poles to great circle trajectories from individual samples are plotted as squares, clearly defining a circle with a pole near the mean directions of individual line fits. Upper hemisphere projections are shown as open symbols. The overall mean is plotted as a star and the expected Eocene reference direction as a square, both with gray confidence intervals. Site means with $\alpha 95 > 15°$ were excluded from the grand mean. The inferred tilt axis with azimuth 230° shows that about 20°of rotation brings the observed direction in perfect agreement with the reference direction.

although visible scatter is evident in some sites. The degree of anisotropy is relatively high, with percent anisotropy values ranging from about 5% to 13.5%. At most sites the magnetic foliation, as defined by the maximum and intermediate susceptibility axes, dips steeply and is closely parallel to the concentric magmatic foliation. Good examples are sites 11 and 12 in the northern part of the pluton, and sites 1, 3 and 4–5 in the western part. The magnetic foliation sites 7, 8 and 9 on the eastern side of the pluton are slightly oblique to magmatic foliation, but a simple explanation for this discordance is not available. A possible explanation is interference of magmatic and tectonic fabrics.

The density of sampling does not allow significant inferences about emplacement mechanisms; this is planned as future work. However, site 6, on the eastern side of the pluton is of particular interest to our discussion. In this site, the orientation of the magnetic foliation is markedly oblique to the magmatic foliation but closely parallels tectonic foliation (Figure 9). This site also shows a strongly oblate fabric, and the maximum and intermediate axes form a girdle distribution, while the minimum susceptibility axis deviates significantly from the horizontal. The fact that magnetic foliation is parallel to the orientation of the mylonitic shear zones is most relevant, because the remanent magnetization is indistinguishable from what is observed at other sites. This further supports the interpretation of the solid-state fabric as comagmatic, as described above. The fabric recorded at site 6 appears to be confined to a small area along the extension of one of the shear zones in the southern part of the pluton.

DISCUSSION

CMB intrusions emplaced into the relatively competent limestones of the Tamaulipas Superior Formation produced deformation aureoles. The aureoles are characterized by isoclinal folds with nearly vertical axial planes, solid-state foliations near the pluton–host rock contact, open folds toward the outer part of these deformation aureoles, and brittle deformation represented by faults and fractures (Cano-González, 2002; Tovar-Cortés, 2002; Terrazas-Calderón, 2002; Valdez-Reyes, 2002). Nonetheless, the pluton–host rock contacts for CMB intrusions vary from highly discordant (*i.e.*, Marcelinos), to nearly concordant (*i.e.*, Cerro Mercado), to markedly concordant (*i.e.*, Cerro Boludo). These variations in structure, fabric, and pluton–host rock relations suggest that there is a complex upper crustal structure beneath the Coahuila fold belt. This structure is likely attributable to variable composition of rocks in the Sabinas basin, lateral facies changes, the presence of evaporites, and a complex basement structure inherited from the time of basin opening. Basement faults may have also assisted in channeling magmatism of the CMB (Chávez-Cabello, 2005).

Cerro Mercado is exceptional among intrusions of the Candela-Monclova magmatic belt, in that most of the plutons do not preserve an obvious magmatic foliation or a solid-state fabric. Cerro Mercado is also considered key to understanding the timing of deformation of the Laramide orogeny in Coahuila, because it is the only pluton of the CMB that contains internal fabrics that suggest it was deformed during and apparently also after emplacement. We further note that Cerro Mercado is the oldest pluton of the CMB, being about 3 Ma older than plutons such as Cerro Boludo, Carrizal and Providencia, which have features typical of post-tectonic intrusions (Chávez-Cabello, 2005).

The relationships between structural features attrib-

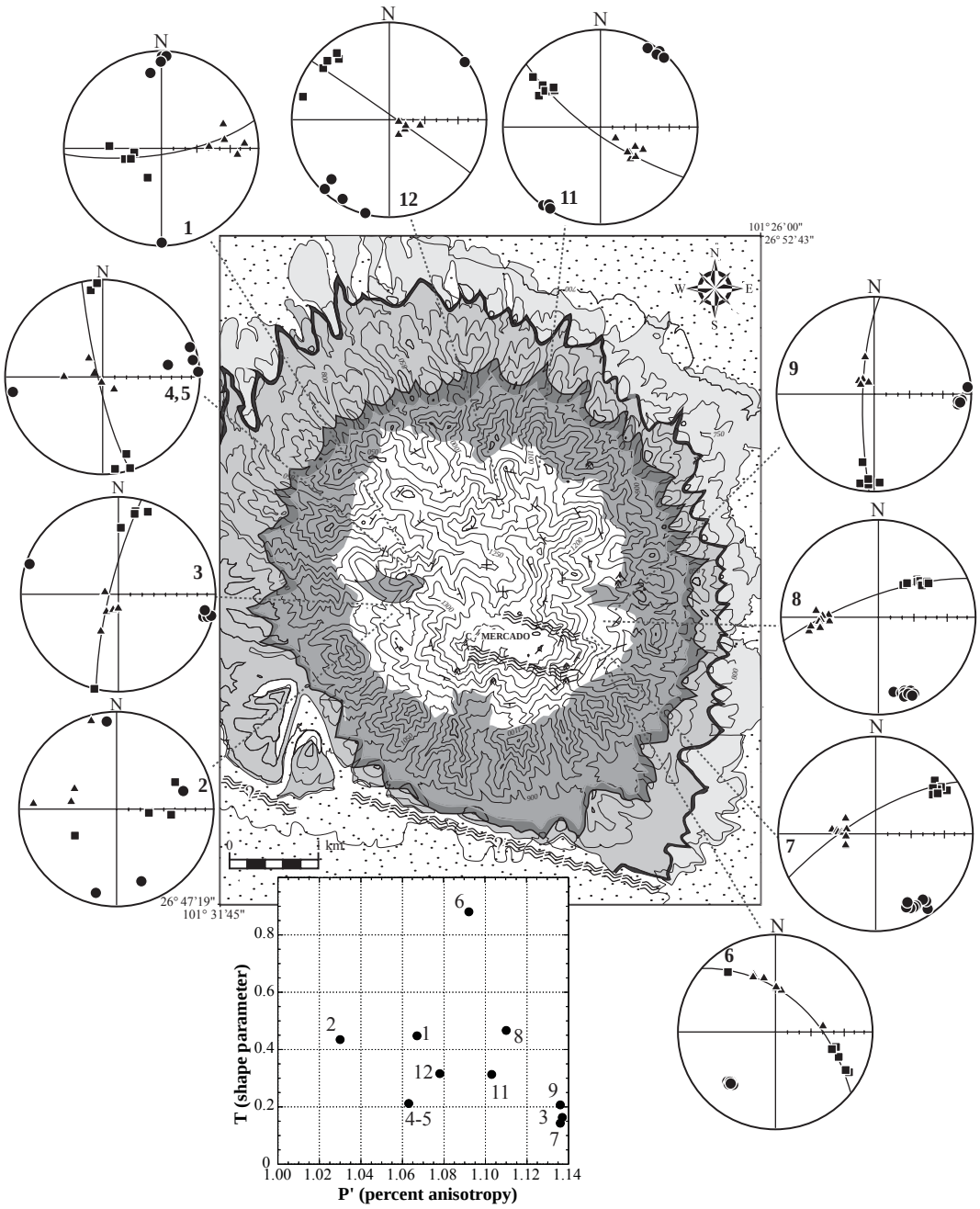

Figure 9. Magnetic anisotropy data for the Cerro Mercado intrusion. Maximum, intermediate and minimum susceptibility axes are plotted as squares, triangles, and circles, respectively. A magnetic foliation plane (solid line) is traced through the maximum and intermediate axes and it is compared with the magmatic foliation (dashed line), except for site 6 where it is compared with the solid-state fabric (dotted line). All projections are in the lower hemisphere; rock units are described in Figure 3. The plot on the lower left is a graph of percent anisotropy (P') *vs.* T (shape parameter).

uted to the Laramide orogeny and to the emplacement and deformation of intrusive rocks of the Candela-Monclova magmatic belt may be used to establish the timing of events leading to culmination of the Laramide orogeny. In this context, data for the CMB are critical, because the contact between synorogenic and postorogenic deposits in La Popa foreland basin of the Laramide belt (Sierra Madre Oriental; Figure 1) in Nuevo León and Coahuila states has been removed by later erosion (Eguiluz de Antuñano, 2001; Gray *et al.*, 2001). The timing of culmination has been bracketed between 45 and 35 Ma (post Ypresian) for La Popa area (Vega-Vera and Perrilliat, 1989; Soegaard *et al.*, 1997; Lawton *et al.*, 2001). It thus includes the range of ages for the CMB. For the Burgos basin, to the east, termination of the Laramide orogeny is estimated at ~39.5 Ma (the age of an unconformity below the Cook Mountain Formation, Eguiluz de Antuñano, 2001).

The Cerro Mercado pluton intruded near the southern

termination of Sierra Sacramento. This range is formed by a complex anticline developed by two deformational phases of the Laramide orogeny, or superposition of two different shortening directions. Its composite fold axis describes a sigmoid, which suggests apparent lateral shear along its northern and southern ends (Figure 2). The structures accommodating lateral shear trend NW-SE to WNW-ESE, but displacement observed in the field is relatively minor. This relationship results in apparent clockwise rotation of Sierra Sacramento, which could indicate that there is a component of right-lateral shear. This component would have to be significant to create this structure.

The mean declination for the pluton indicates a (statistically insignificant) apparent clockwise rotation of 8.0°±15.6°. Paleomagnetic data may thus be interpreted to support the rotation inferred from field relations. Nonetheless, rotation about a vertical axis alone does not fully explain the discordant mean paleomagnetic direction. The mean inclination (61.3°) indicates that the pluton has been tilted (down to the north) about 20°.

The rotation indicated by the discordant declinations is small compared with the difference in fold axis trends at Sierra Sacramento. Furthermore, only small displacement was observed on NW striking faults. Thus, the simplest interpretation of the discordant direction requires a simple tilt down to the northwest, which explains both the apparent rotation and the steepening of inclination without invoking a significant component of lateral shear. For instance, restoring 20° of tilt along a SW-NE axis (230° azimuth), brings the observed mean to coincide with the expected Eocene direction (Figure 8). NW-down tilt of the pluton is consistent with truncation of the Upper Cretaceous sequence along the southern margin of the pluton (Figure 3). Also, the pluton is affected by WNW striking right-lateral ductile structures (Figure 4), which may have also accommodated some degree of tilt.

We acknowledge that given the relatively small size of the pluton, the small size of the paleomagnetic data set, and the near uniform polarity of the magnetization observed, we cannot fully discount that the paleomagnetic discordance is due to incomplete averaging of paleosecular variation. But we would argue that the presence of dual polarities at one site and an acceptable angular dispersion for the sampling paleolatitude suggest that the discordance cannot be explained solely on that basis. Furthermore, slow cooling may have contributed to average some secular variation at the site level.

The overall mean is based on samples of a single polarity, thus incomplete isolation of a ChRM may bias the final result. If this was the case, the estimate of tilt (~20º) must be considered a minimum estimate. As explained above, contamination of the reverse polarity ChRM by the normal polarity overprint would result in shallower mean inclination.

There is considerable debate on the interpretation of structural fabrics in plutons in relation to the timing of emplacement relative to deformation. Key observations at Cerro Mercado are: the existence of magmatic and ductile fabrics and evidence that ductile fabrics are comagmatic. We also note the apparent interaction of the pluton with the anticline of Sierra Sacramento. These observations suggest a syntectonic emplacement.

We note that the rate of cooling derived from Ar-Ar data is slow for a relatively small pluton. The exposed area represents only part of the pluton, but even allowing for a slightly larger pluton as suggested by aeromagnetic data (Servicio Geológico Mexicano, 2000) the rate is still slow. Gray *et al.* (2001) data on burial depths of Mesozoic strata would suggest emplacement at about 5 km. It is thus likely that Cerro Mercado was emplaced into relatively 'hot" rocks during times of a greater geothermal gradient. The limited development of a contact metamorphism aureole around the pluton, and its phaneritic texture, support slow cooling and intrusion into a relatively "hot" host rock.

A model for the structural evolution of Cerro Mercado needs to explain tilt of the pluton (or combined small clockwise rotation and tilt), localized plastic deformation fabrics, a magmatic foliation, and other field relations already described. Tilt (of the pluton and its host rock) may be explained by normal faulting, which would require north-south extension in order to tilt the pluton to the north, as long as the pluton is seated on the hanging wall of a normal fault that flattens at depth. There is, however, no structural evidence of significant Cenozoic age normal faulting in the Sabinas basin. Structures in and around the pluton are consistent with NNE contraction and localized strike-slip (Figure 3) due to a complex architecture of the basement faults. Left-lateral faults north and south of Sierra Sacramento (Figure 2) are relatively minor compared to right-lateral faults in the pluton and in the host rock south of it (Figure 3). Also, seismic profiles in the Sabinas basin show structures interpreted as basement reverse faults (R. Paterson, personal communication, 2006; Eguiluz de Antuñano *et al.*, 2000). North-south extension does not, therefore, provide a satisfactory explanation.

We propose that deformation related to basin inversion provides a more suitable explanation. It has been proposed that fault inversion may occur by two general mechanisms (Buchanan and McClay, 1991): inversion without tilt of basement blocks and inversion with tilt of basement blocks. Both mechanisms produce shear on the fault plane and vertical stress on the overlying sequence, developing drape folds and/or tilt in rigid bodies (Figure 10). In our interpretation, the paleomagnetic discordance and tilt of the Cerro Mercado pluton resulted from rotation about a horizontal axis that in turn was caused by shear along a high-angle fault during inversion of basement faults in the southern margin of the Sabinas basin during a late phase of Laramide deformation in the area (Figure 10). We thus propose that normal basement faults formed in Triassic-Jurassic time assisted in channeling magmatism of the CMB, these same faults were inverted during Laramide time, and

may have controlled ductile and brittle deformation present at Cerro Mercado. We thus suggest that the mechanism of inversion of basement blocks is responsible for tilt of the Cerro Mercado pluton.

The structural and paleomagnetic data suggest that the pluton was deformed in the general contractional deformation field during Laramide orogenesis. Also, magnetic fabrics suggest that solid-state fabrics at Cerro Mercado are comagmatic. Thus, as indicated by $^{40}Ar/^{39}Ar$ geochronological data, the Laramide orogeny in the Coahuila fold belt ended after intrusion of the Cerro Mercado pluton *ca.* 44 Ma, the best approximation for the time of remanent magnetization acquisition.

REGIONAL IMPLICATIONS

The Coahuila fold belt is structurally and kinematically different from the Sierra Madre Oriental (SMO) fold and thrust belt (Ye, 1997; Eguiluz de Antuñano *et al.*, 2000). Initially, deformation in the Coahuila fold belt was attributed to transpression (Charleston, 1981; Padilla y Sánchez, 1982, 1986), and later to combined mechanisms such as detachment and basin inversion (Chávez-Cabello, 2005). In contrast, the SMO fold and thrust belt is characterized mainly by detachments and less important basement fault reactivation, also with development of structural salients. Proposed syn-Laramide rotation of the Coahuila block may have contributed to transpression in the Coahuila fold belt (Molina-Garza, 2005).

The oblique trend of the CMB intrusives to the Laramide structural grain, the well defined trend of magmatism, and pluton emplacement at shallow levels within the Sabinas basin suggest, as a first approximation, a strong mechanical control to magma ascent. On the basis of the scale of the CMB, its regional trend is unlikely to reflect only details within the Mesozoic sequence. Additional control was likely exerted by structures in the basement, and possibly by differential stress. Control on magma ascent may have been exerted by neutral buoyancy forces compared to the Upper Jurassic evaporite sequence along the northern margin of the Coahuila fold belt and by intersection of highly fractured calcareous rocks (Lister and Kerr, 1991). Evaporite distribution also exerted an important control on styles of deformation (Padilla y Sánchez, 1986).

In general, most intrusions of the CMB are post-tectonic with respect to an earlier Laramide phase of detachment folds (Cano-González, 2002; Tovar-Cortés, 2002; Valdez-Reyes, 2002), but our data show that Cerro Mercado was emplaced during a later phase of reactivation of basement faults, tectonic inversion, and generation of sigmoidal structures. Furthermore, we infer that fault reactivation facilitated magma ascent to shallow crustal levels.

Although a full review of the Laramide orogeny in northern Mexico is beyond the scope of this contribution, we may summarize the following observations. In the interval between 80 and 45 Ma there is a clear eastward migration of arc magmatism in northern Mexico (Damon *et al.*, 1981; Clark *et al.*, 1982; McDowell *et al.*, 2001). The onset of Laramide deformation is marked by crustal shortening, emplacement of magmas in the lower series of the Sierra Madre Occidental, and changes in sedimentary facies in central and northeast Mexico (Eguiluz de Antuñano and Campa, 1982). Uplift in the west triggered regional *décollement* of the Mesozoic sequence of northeast Mexico above favorable surfaces. This phase of deformation culminated with thrusting of the Mesozoic sequence above basement highs in Chihuahua, Coahuila, and segments of the fold belt south of Monterrey (Ye, 1997). For central Coahuila this phase of *décollement* is evident along the trace of the San Marcos fault (Chávez-Cabello *et al.*, 2005).

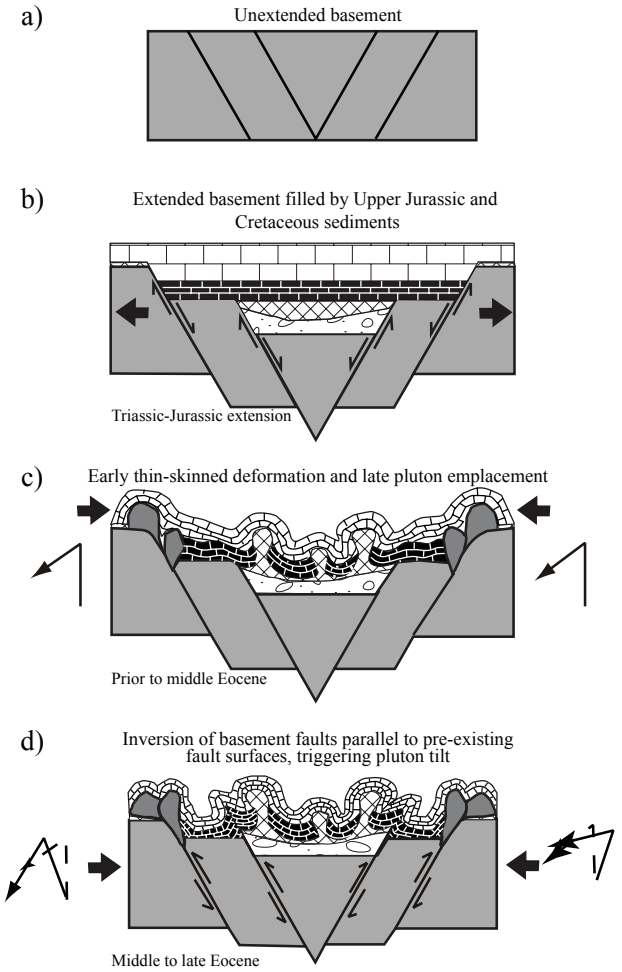

Figure 10. Diagrammatic model showing, in stages, the structural evolution of the Sabinas basin and the Cerro Mercado monzonite. a: pre-Mesozoic basement unextended; b: basement extension and basin fill with Upper Triassic (?) – Jurassic continental clastic strata, and Upper Jurassic – Cretaceous marine sediments; c: early Laramide thin-skinned deformation and middle-Eocene pluton emplacement; d: basement fault inversion during a late phase of Laramide deformation and pluton tilt. Solid and dashed arrows show, respectively, the inclination of the magnetization vector upon cooling and after tilt.

For the critical interval between 46 and ~35 Ma, the Farallon slab must have attained its lowest subduction angle, with the consequent migration of arc volcanism into Coahuila's Candela-Monclova belt. We hypothesize that reactivation of the San Marcos fault and other basement faults represent the last manifestation of shortening produced by the Laramide orogeny at this time. This was a short episode of deformation that ended by the time of emplacement of younger plutons of the CMB *ca.* 41 Ma (Chávez-Cabello, 2005).

The studies of McBride *et al.* (1974) in the Parras Basin and Vega-Vera and Perrilliat (1989) in La Popa basin suggest that the orogeny had ended by late Eocene time. A more precise age cannot be established biostratigraphically as the youngest synorogenic sediments of La Popa basin lack age diagnostic fossils. In the Burgos basin (Figure 1, inset), there is a strong discordance at the top of the Cook Mountain Formation (Ortiz-Ubilla and Tolson, 2004). Overlying these units are the Yegua and Jackson formations, a wedge of transgressive-regressive sequences of the upper Eocene (~39.5 Ma) interpreted as the culminating event of the Laramide orogeny in the Burgos basin (Eguiluz de Antuñano, 2001).

Although shortening directions are not necessarily diagnostic of age, because geometry may be affected by rocks such as evaporites, according to De Cserna (1956), Tardy (1980), Ye (1997), and Soegaard *et al.* (2003), an earlier Laramide episode of north to north-northeast shortening in the Sierra Madre Oriental ended by the Paleocene-Eocene boundary, because east-west trending faults and folds characteristic of the region between Torreón and Monterrey are not present in the Eocene sequence of La Popa basin. Rocks in La Popa basin and the Coahuila fold belt record (younger) northeast-directed shortening. Because the youngest plutons of the CMB cut NW-SE oriented folds, they provide the best means to date this late phase of the Laramide orogeny between about 44 and 41 Ma.

CONCLUSIONS

The Cerro Mercado pluton contains magmatic, ductile, and brittle fabrics that suggest a combination of local and regional imposed stresses. Tectonic foliation at Cerro Mercado is parallel to WNW oriented shear zones. Magnetic fabric and paleomagnetic data support interpretation of the mylonite as comagmatic. A hornblende mineral separate from the pluton yielded a $^{40}Ar/^{39}Ar$ plateau age at 44.29 ± 0.19 Ma. This age is a cooling age, and represents a minimal age for crystallization of the monzonite intrusion. A biotite total fusion age at 41.23 ± 0.21 Ma is interpreted as the time when the monzonite intrusive cooled below ~280 ± 40°C, the closure temperature of biotite. These age constraints suggest relatively slow cooling of the Cerro Mercado pluton (rate of ~80 °C/Ma between hornblende and biotite). Paleomagnetic data for the pluton yield well-defined remanent magnetizations of nearly uniform reverse polarity, with a grand mean of D=178.2° and I=-61.7° (N=9 sites). The mean is statistically discordant with respect to the Eocene reference direction of North America in inclination and declination. The simplest interpretation of these data attributes the discordance to northwestward tilt of the pluton during basin inversion, although the alternative of tilt and clockwise rotation within a weakly right-lateral transpressive regime with NNW directed compression cannot be excluded. The strain field is consistent with contraction during the Laramide orogeny. The pluton is thus syntectonic, indicating that the Laramide orogeny in central Coahuila ended some time after ~44 Ma (the minimum age estimate for the Cerro Mercado pluton) but before ~41 Ma (the age of younger postectonic plutons of the Candela-Monclova belt).

ACKNOWLEDGEMENTS

This research was supported by CONACYT through grant 47071 to JJAG and collaborators. Iriondo is very thankful to Mick Kunk for his guidance while running the $^{40}Ar/^{39}Ar$ samples at the USGS Thermochronology Lab in Denver. Tim DeBay and the staff of the U.S. Geological Survey TRIGA reactor in Denver are greatly thanked for supplying the right dose of neutrons to activate our geological samples to perform the $^{40}Ar/^{39}Ar$ geochronology. Roy George (USGS) is greatly acknowledged for his help preparing the mineral separates for geochronology. We also thank the comments on earlier versions of this manuscript of Scott Johnson, Elizabeth Nagy-Shadman, Steve Harlam, Augusto Rapalini, Randall Marrett, Timothy Lawton, and Arturo Martín-Barajas.

APPENDIX. ^{40}Ar-^{39}Ar ANALYTICAL TECHNIQUES

Hornblende and biotite mineral separates from two monzonite samples from Cerro Mercado (M-23 and M27; Figure 3) were obtained at the U.S. Geological Survey in Denver for $^{40}Ar/^{39}Ar$ geochronology studies. The separates ranged in size between 250 and 125 μm, and were obtained using magnetic separation, heavy liquids, and hand picking techniques to a purity of >99%.

Aliquots of hornblende and biotite from both rock samples were packaged in copper capsules and sealed under vacuum in quartz tubes. The samples were then irradiated for 16 hours (package KD25) in aluminum containers in the central thimble facility at the TRIGA reactor (GSTR) at the U.S. Geological Survey in Denver, Colorado. The monitor mineral used for the different irradiations was Fish Canyon Tuff (FCT-3) sanidine with an age of 27.79 Ma (Kunk *et al.*, 1985; Cebula *et al.* 1986) relative to MMhb-1 with a K-Ar age of 519.4 ± 2.5 Ma (Alexander *et al.*, 1978; Dalrymple *et al.*, 1981). The type of container and the geometry of

samples and standards are similar to that described by Snee *et al.* (1988).

All of the samples were analyzed at the U.S. Geological Survey Thermochronology Laboratory in Denver, Colorado using a VG Isotopes Ltd., Model 1200B mass spectrometer fitted with an electron multiplier. We used the $^{40}Ar/^{39}Ar$ furnace step-heating method to determine the age of the mineral separates. In addition, a second aliquot of biotite for sample M-27 (#95KD25) was analyzed using the total fusion method, whereby the sample is totally melt (fused) in a single temperature step in the furnace at ~1450°C. For additional information on the analytical procedure for both techniques see Kunk *et al.* (2001) and Iriondo *et al.* (2003, 2004).

All the argon step-heating and the total fusion isotopic data were reduced using an updated version of the computer program ArAr* (Haugerud and Kunk, 1988) an are presented at the 1σ level of analytical precision in Table 1. The step-heating experiments are presented as age spectrum diagrams as well as inverse isotope correlation diagrams in Figure 5. The decay constants used in the calculations are those recommended by Steiger and Jäger (1977). Inverse isotope correlation analysis of the step-heating data was used to assess if non-atmospheric argon components were trapped in any samples and to calculate an inverse isochron age using the method of York (1969). For additional information on the sample data reduction procedure see Haugerud and Kunk (1988). Plateau ages, reported at the 1σ level of precision in Table 1 and Figure 5, are identified when three or more contiguous steps in the age spectrum agree in age, within the limits of analytical precision (1σ), and contain more than 50% of the $^{39}Ar_K$ released from the sample (Fleck *et al.*, 1977). Only the apparent ages in the age spectrum diagrams (Figure 5) are plotted at the 2σ level of precision, but just for graphical purposes to improve visual assessment of the data. Total gas ages, shown in Table 1 and Figure 5b, represent the age calculated from the integration of all the $^{40}Ar/^{39}Ar$ step-heating age results for the sample into a one single age value; the total gas ages are thus roughly equivalent to conventional K-Ar ages. No analytical precision is calculated for the total gas ages because this analytical uncertainty does not, by any means, represent the total geological uncertainty in the age of the mineral and/or rock.

REFERENCES

Alexander, E.C., Jr., Mickelson, G.M., Lanphere, M.A., 1978, Mmhb-1: a new $^{40}Ar/^{39}Ar$ dating standard, *in* Zartman, R.E., (ed.), Short papers of the fourth international conference, geochronology, cosmochronology, and isotope geology: U.S. Geological Survey, Open-File Report 78-701, 6-8.

Aranda-Gómez, J.J., Housh, T.B., Luhr, J.F., Becker, T., Solorio-Munguía, J.G., Martínez, E., 2001, Timing of multiepisodic deformation based on the study of continental clastic deposits and volcanic rocks, east-central Chihuahua, México: GEOS, 21(3), 204.

Aranda-Gómez, J.J., Luhr J. F., Housh, T. B., Valdez-Moreno, G., Chávez-Cabello, G., 2005, El volcanismo tipo intraplaca del Cenozoico tardío en el centro y norte de México: una revisión: Boletín Sociedad Geológica Mexicana, 57(3), 187-226.

Arvizu-Gutiérrez, I., 2006, Paleomagnetismo de rocas jurásicas y cretácicas del Valle San Marcos, Coahuila, México: Querétaro, México, Universidad Nacional Autónoma de México, Posgrado en Ciencias de la Tierra, Tesis de Maestría, 139 p.

Bailey, R.C., Halls, H.C., 1984, Estimate of confidence in paleomagnetic directions derived from mixed remagnetized circle and direct observation data: Journal of Geophysics, 54, 174-182.

Bird, P., 2002, Stress direction history of the western United States and Mexico since 85 Ma: Tectonics, 21, 5-12.

Brun, J.P, Pons, J., 1981, Strain patterns of pluton emplacement in crust undergoing non-coaxial deformation, Sierra Morena, southern Spain: Journal of Structural Geology, 3, 219-230.

Buchanan, P.G., McClay, K.R., 1991, Sandbox experiments of inverted listric and planar faults systems, *in* Cobbold, P.R. (ed.), Experimental and Numerical Modeling of Continental Deformation: Tectonophysics, 188, 97-115.

Bunge, H.P., Grand, S.P., 2000, Mesozoic plate motion history below the northeast Pacific ocean from seismic images of the subducted Farallon slab: Nature, 405, 337-340.

Cande, S.C., Kent, D.V., 1995, Revised Calibration of the geomagnetic polarity time scale: Journal of Geophysical Research, 100, 6093-6095.

Cano-González, A., 2002, Geología y geoquímica del intrusivo Cerro La Soledad, margen oriental del Cinturón Candela Monclova, Provincia Alcalina Oriental Mexicana: Linares, Nuevo León, Universidad Autónoma de Nuevo León, Facultad de Ciencias de la Tierra, Tesis de Licenciatura, 113 p.

Cebula, G.T., Kunk, M.J., Mehnert, H.H., Naeser, C.W., Obradovich, J.D., Sutter, J.F., 1986, The Fish Canyon Tuff: A potential standard for the $^{40}Ar/^{39}Ar$ and fission track dating methods: Terra Cognita, 6(2), 139-140.

Charleston, S., 1981, A summary of the structural geology and tectonics of the State of Coahuila, Mexico, *in* Schmidt, C.I., Katz, S.B. (eds.), Lower cretaceous stratigraphy and structure, northern Mexico: West Texas Geological Society Field Trip Guidebook, Publication 81-74, 28-36.

Chávez-Cabello, G., 2005, Deformación y magmatismo cenozoicos en sur de la cuenca de Sabinas, Coahuila, México: Querétaro, México, Universidad Nacional Autónoma de México, Posgrado en Ciencias de la Tierra, Ph.D. Thesis, 266 p.

Chávez-Cabello, G., Aranda-Gómez, J.J., Molina-Garza, R.S., Cossío-Torres, T., Arvizu-Gutiérrez, I.R., González-Naranjo, G., 2005, La Falla San Marcos: Una estructura jurásica de basamento multi-reactivada del noreste de México, *in* Alaniz-Álvarez, S.A., Nieto-Samaniego, A.F. (eds.), Grandes Fronteras Tectónicas de México: Boletín de la Sociedad Geológica Mexicana, Volumen Conmemorativo del Centenario, 57(1), 27-52.

Clark, K.F., Foster, C.T., Damon, P.E., 1982, Cenozoic mineral deposits and subduction related arcs in northern Mexico: Geological Society of America Bulletin, 93, 533-544.

Courrioux, G., 1987, Oblique diapirism: the Criffel granodiorite/granite zoned pluton (southwest Scotland): Journal of Structural Geology, 9, 313-330.

Damon, P.E., Shafiqullah, M., Clark, K.F., 1981, Age trends of igneous activity in relation to metallogenesis in the southern Cordillera: Arizona Geological Society Digest, 14, 137-154.

Dalrymple, G.B., Alexander, E.C., Lanphere, M.A., Kraker, G.P., 1981, Irradiation of samples for $^{40}Ar/^{39}Ar$ dating using the Geological Survey TRIGA reactor: U.S. Geological Survey Professional Paper 1176, 55 p.

De Cserna, Z., 1956, Tectónica de la Sierra Madre Oriental de México entre Torreón y Monterrey: México D.F., XX Congreso Geológico Internacional, Monografía, 60 p.

Demarest, H.H., 1983, Error analysis for the determination of tectonic rotation from paleomagnetic data: Journal of Geophysical Research, 88, 4321-4328.

Diehl, J.F., McClannahan, K.M., Bornhorst, T.J., 1988, Paleomagnetic

results from the Mogollon-Datil volcanic field, southwestern New Mexico and a refined Mid-Tertiary reference pole for North America: Journal of Geophysical Research, 93, 4869-4879.

Dunlop, D.J., Schmidt, P.W., Ozdemir, O., Clark, D.A., 1997, Paleomagnetism and paleothermometry of the Sydney Basin; 1. Thermoviscous and chemical overprinting of the Milton Monzonite: Journal Geophysical Research, 102, 27,271-27,283.

Eguiluz de Antuñano, S., 2001, Geologic evolution and gas resources of the Sabinas basin in northeastern México, *in* Bartolini, C., Buffler, R.T., Cantú-Chapa, A. (eds.), The Western Gulf of México Basin: Tectonics, Sedimentary Basins, and Petroleum Systems: American Association of Petroleum Geologists, Memoir 75, 241-270.

Eguiluz de Antuñano, S., Campa, M.F., 1982, El geosinclinal mexicano en el sector de San Pedro Gallo, Durango, *in* VI Convención Nacional de la Sociedad Geológica Mexicana, Libro de Resúmenes, p. 3.

Eguiluz de Antuñano, S., Aranda, G.M., Marrett, R., 2000, Tectónica de la Sierra Madre Oriental, México: Boletín de la Sociedad Geológica Mexicana, 53, 1-26.

Fisher, R.A., 1953, Dispersion on a sphere: Proceedings of the Royal Society of London, A 217, 295-305.

Fleck, R.J., Sutter, J.F., Elliot, D.H., 1977, Interpretation of discordant $^{40}Ar/^{39}Ar$ age spectra of Mesozoic tholeiites from Antarctica: Geochimica et Cosmochimica Acta, 41, 15-32.

Gilmer, A.K., Kyle, J.R., Connelly, J.N., Mathur, R.D., Henry, C.D., 2003, Extension of Laramide magmatism in southwestern North America into Trans-Pecos Texas: Geology, 31(5), 447-450.

Goldhammer, R.K., 1999, Mesozoic sequence stratigraphy and paleogeographic evolution of northeast of Mexico, *in* Bartolini, C., Wilson, J.L., Lawton, T.F. (eds.), Mesozoic Sedimentary and Tectonic History of North-Central Mexico: Boulder, Colorado, Geological Society of America, Special Paper 340, 1-58.

González-Naranjo, G., 2006, Análisis estructural y estudio paleomagnético en Potrero el Colorado, Coahuila, México: Linares, Nuevo León, Universidad Autónoma de Nuevo León, Facultad de Ciencias de la Tierra, Tesis de Maestría, 221 p.

Gray, G.G., Pottorf, R.J., Yurewicz, D.A., Mahon, K.I., Peaver, D.R., Chuchla, R.J., 2001, Thermal and chronological record of Syn- to Post-Laramide burial and exhumation, Sierra Madre Oriental, Mexico, *in* Bartolini, C., Buffler, R.T., Cantú-Chapa, A. (eds.), The Western Gulf of Mexico Basin: Tectonics, Sedimentary Basins, and Petroleum Systems: American Association of Petroleum Geologists, Memory 75, 159-181.

Guineberteau, B., Bouchez, J.L., Vigneresse, J.L., 1987, The Mortagne granite pluton (France) emplaced by pull-apart along a shear zone: structural and gravimetric arguments and regional implications: Geological Society of America Bulletin, 99, 763-770.

Harlan, S., Geissman, H.W., Henry, C.D., Onstott, T.C., 1995, Paleomagnetism and ^{40}Ar-^{39}Ar geochronology of gabbro sills at Mariscal Mountain anticline, southern Big Bend National Park, Texas: Implications for the timing of Laramide tectonism and vertical axis rotations in the southern Cordilleran orogenic belt: Tectonics, 14, 307-321.

Harrison, T.M., 1981, Diffusion of ^{40}Ar in hornblende: Contributions to Mineralogy and Petrolology, 78, 324-331.

Harrison, T.M., Duncan, I., McDougall, I., 1985, Diffusion of ^{40}Ar in biotite: Temperature, pressure and compositional effects: Geochimica et Cosmochimica Acta, 49, 2461-2468.

Haugerud, R.A., Kunk, M.J., 1988, ArAr*, a computer program for reduction of ^{40}Ar-^{39}Ar data: U.S. Geological Survey, Open-File Report 88-261, 68 p.

Henry, C.D., Price, J.G., James, E.W., 1991, Mid-Cenozoic Stress Evolution and Magmatism in the Southern Cordillera, Texas and Mexico: Transition from Continental Arc to Intraplate Extension: Journal of Geophysical Research, 96, 13,545-13,560.

Hess, J.C., Lippolt, H.J., Wirth, R., 1987, Interpretation of $^{40}Ar/^{39}Ar$ spectra of biotites: Evidence from hydrothermal degassing experiments and TEM studies: Chemical Geology, 66, 137-149.

Holder, M. T., 1979, An emplacement mechanism for post-tectonic granites and its implications for their geochemical features, *in* Atherton, P.P., Tarney, J. (eds.), Origin of Granite Batholiths —Geochemical Evidence: Orpington, U.K., Shiva Publishers, 116-128.

Hutton, D.W.H., 1981, The Main Donegal granite: lateral wedging in a synmagmatic shear zone (abstract): Journal of Structural Geology, 3, p. 93.

Iriondo, A., Kunk, M.J., Winick, J.A., Consejo de Recursos Minerales, 2003, $^{40}Ar/^{39}Ar$ dating studies of minerals and rocks in various areas in Mexico: USGS/CRM Scientific Collaboration (Part I): U.S. Geological Survey Open File Report, OF-03-020, 79 p.

Iriondo, A., Kunk, M.J., Winick, J.A., Consejo de Recursos Minerales, 2004, $^{40}Ar/^{39}Ar$ dating studies of minerals and rocks in various areas in Mexico: USGS/CRM Scientific Collaboration (Part II): U.S. Geological Survey Open File Report, OF-04-1444, 46 p.

Iriondo, A., Martínez-Torres, L.M., Kunk, M.J., Atkinson, W.W., Jr., Premo, W.R., McIntosh W.C., 2005, Northward Laramide thrusting in the Quitovac region, northwestern Sonora, Mexico: Implications for the juxtaposition of Paleoproterozoic basement blocks and the Mojave-Sonora megashear hypothesis, *in* Anderson, T.H., Nourse, J.A., McKee, J.W., Steiner, M.B. (eds.), The Mojave-Sonora Megashear Hypothesis: Development, Assessment, and Alternatives: Geological Society of America, Special Paper 393, 631-669.

James, E.W., Henry, C.D., 1991, Compositional changes in Trans-Pecos Texas magmatism coincident with Cenozoic stress realignment: Journal Geophysical Research, 96, 13,561-13,575.

Kirschvink, J.L., 1980, The least square line and plane and the analysis of paleomagnetic data: Geophysical Journal of the Royal Astronomical Society, 62, 699-718.

Kleist, A., Hall, S.A., Evans, I., 1984, A paleomagnetic study of the Lower Cretaceous Cupido Limestone, northeast Mexico: Evidence for local rotation within the Sierra Madre Oriental: Geological Society of America Bulletin, 95(1), 55-60.

Kunk, M.J., Sutter, J.F., Naeser, C.W., 1985, High-precision $^{40}Ar/^{39}Ar$ ages of sanidine, biotite, hornblende, and plagioclase from the Fish Canyon Tuff, San Juan Volcanic Field, south-central Colorado: Geological Society of America, Abstracts with Programs, 17, 636.

Kunk, M.J., Winick, J.A., Stanley, J.O., 2001, $^{40}Ar/^{39}Ar$ age-spectrum and laser fusion data for volcanic rocks in west central Colorado: U.S. Geological Survey, Open-File Report 01-472, 94 p.

Lamourux, C., Soyula, J.C., Deramond, J., Roddaz, B., 1980, Shear zones in the granodioritic massifs of the central Pyrinees and the behavior of these massifs during Alpine orogenesis: Journal of Structural Geology, 2, 49-53.

Lawton, T.F., Vega-Vera, F.J., Giles, K.A., Rosales-Domínguez, C., 2001, Stratigraphy and origin of the La Popa basin, Nuevo Leon and Coahuila, Mexico, *in* Bartolini, C., Buffler, R.T., Cantú-Chapa, A. (eds.), The Western Gulf of Mexico Basin: Tectonics, Sedimentary Basins, and Petroleum Systems: American Association of Petroleum Geologists, Memory 75, 219-240.

Lister, J.R., Kerr, R.C., 1991, Fluid-mechanical models of crack propagation and their application to magma transport in dykes: Journal of Geophysical Research, 96: 10,049-10,077.

McBride, E.F., Weidie, A.E., Wolleben, J.A., Laudon, R.C., 1974, Stratigraphy and structure of the Parras and La Popa basins, northeastern Mexico: Geological Society of America Bulletin, 85, 1603-1622.

McDougall, I., Harrison, T.M., 1999, Geochronology and Thermochronology by the $^{40}Ar/^{39}Ar$ method: New York, Oxford University Press, 288 p.

McDowell, F.W., Roldán-Quintana, J., Connelly, J.N., 2001, Duration of Late Cretaceous-early Tertiary magmatism in east-central Sonora, Mexico: Geological Society of America Bulletin, 113, 521-531.

McFadden, P.L., McElhinny, M.W., 1984, A physical model for palaeosecular variation: Geophysical Journal of the Royal Astronomical Society, 78, 809-830.

McFadden, P.L., McElhinny, M.W., 1988, The combined analysis of remagnetization circles and direct observations in paleomagnetism, Earth and Planetary Science Letters, 87, 161-172.

McKee, J.W., Jones, N.W., Long, L.E., 1990, Stratigraphy and provenance of strata along the San Marcos fault, central Coahuila, Mexico:

Geological Society of America Bulletin, 102, 593-614.
Molina-Garza, R.S., 2005, Paleomagnetic data for the Late Triassic Acatita intrusives, Coahuila, México: Tectonic Implications: Geofísica Internacional, 44, 197-210.
Morton-Bermea, O., 1995, Zur Petrologie des Alkali-Intrusivkomplexes der Sierra de Picachos (Nuevo León, Mexiko): Karlsruhe, Germany, Universität Karlsruhe, Diplomarbeit, 114 p.
Nairn, A.E.M., 1976, A paleomagnetic study of certain Mesozoic formations in northern Mexico: Physics of the Earth and Planetary Interiors, 13, 46-56.
Nowicki, M. J., Hall, S. A., Evans, I., 1993, Palaeomagnetic evidence for local and regional post-Eocene rotations in northern Mexico, Geophysical Journal International, 114, 63-75.
Oliver, N., Wall, V., 1987, Metamorphic plumbing system in Proterozoic calc-silicates, Queensland, Australia: Geology, 15, 793-796.
Ortiz-Ubilla, A., Tolson, G., 2004, Interpretación estructural de una sección sísmica en la región Arcabuz-Culebra de la Cuenca de Burgos, NE de México: Revista Mexicana de Ciencias Geológicas, 21, 226-235.
Padilla y Sánchez, R.J., 1982, Geologic evolution of the Sierra Madre Oriental between Linares, Concepción del Oro, Saltillo and Monterrey, México: University of Texas at Austin, Ph.D. Thesis, 217 p.
Padilla y Sánchez, R.J., 1986, Post Paleozoic tectonics of northeast México and its role in the evolution of the Gulf of México: Geofísica Internacional, 25, 157-206.
Paterson, S.R., Tobisch, O.T., 1988, Using ages to date regional deformations: problems with commonly used criteria: Geology, 16, 1108-1111.
Paterson, S.R., Brudos, T., Fowler, T.K. Jr., Carlson, C., Bishop, K., Vernon, R.H., 1991, Papoose Flat pluton: forceful expansion or post-emplacement deformation?: Geology, 19, 324-327.
Pignotta, G.S., Benn, K, 1999, Magnetic fabric of the Barrington Passage pluton, Meguma terrane, Nova Scotia: a two stage fabric history of syntectonic emplacement: Tectonophysics, 307, 75-92.
Pitcher, W.S., 1979, The nature, ascent and emplacement of granitic magmas: Journal of the Geological Society of London, 136, 627-662.
Ramsay, J. G., 1989, Emplacement kinematics of a granite diapir. The Chindamora batholith, Zimbabwe: Journal of Structural Geology, 11, 191-210.
Reyes-Cortés, I.A., Goodell, P.C., 2000, Geologic setting and mineralization: Sierra Peña Blanca, Chihuahua, Mexico, *in* Cuarta Reunión sobre Geología del Noroeste de México y Áreas Adyacentes: Universidad Nacional Autónoma de México, Instituto de Geología, Estación Regional del Noroeste, Publicaciones Ocasionales, 2, 101.
Robin, C., Tournon, J., 1978. Spatial relations of andesitic and alkaline provinces in Mexico and Central America: Canadian Journal of Earth Sciences, 15, 1633-1641.
Sager, W.W., Mortera-Gutiérrez, C.A., Urrutia-Fucugauchi, J., 1992, Paleomagnetic evidence of Tertiary tectonic rotation in west Texas: Geology, 20, 935-938.
Servicio Geológico Mexicano, 2000, Carta magnética de campo total Monclova G14-4, Scale 1:250,000: Pachuca, Servicio Geológico Mexicano, 1 map.
Sewell, C.R., 1968, The Candela and Monclova belts of igneous intrusions, a petrographic province in Nuevo León and Coahuila, Mexico: Annual Meeting of the Geological Society of America, Abstracts with Programs, p. 273.
Snee, L.W., Sutter, J.F., Kelly, W.C., 1988, Thermochronology of economic mineral deposits: Dating the stages of mineralization at Panasqueira, Portugal, by high precision $^{40}Ar/^{39}Ar$ age spectrum techniques on muscovite: Economic Geology, 83, 335-354.
Soegaard, K., Giles, K.A., Vega-Vera, F.J., Lawton, T.F., 1997, Structure, stratigraphy, and paleontology of Late Cretaceous-Early Tertiary Parras-La Popa foreland basin near Monterrey, northeast Mexico: American Association of Petroleum Geologists Guidebook to Fieldtrip 10, 136 p.
Soegaard, K., Ye, H., Halik, N., Daniels, A.T., Arney, J.. Garrick, S., 2003, Stratigraphic evolution of latest Cretaceous to early Tertiary Difunta foreland basin in northeast Mexico; influence of salt withdrawal on tectonically induced subsidence by the Sierra Madre Oriental fold and thrust belt, *in* Bartolini, C, Buffler, R.T., Blickwede, J.F. (eds.), The Circum-Gulf of Mexico and the Caribbean; Hydrocarbon Habitats, Basin Formation, and Plate Tectonics: American Association of Petroleum Geologists, Memoir 79, 364-394.
Steiger, R.H., Jäeger, E., 1977, Subcommission on geochronology: Convention on the use of decay constants in geo- and cosmochronology: Earth and Planetary Science Letters, 36, 359-363.
Sylvester, A. G., Oertel, G., Nelson, C. A., Christie, J. M., 1978, Papoose Flat Pluton: a granite blister in the Inyo Mountains, eastern California: Geological Society of American Bulletin, 89, 1205-1219.
Symons, D.T.A., Erdmer, P., and McCausland, 2003, New 42 Ma cratonic North American Paleomagnetic pole from the Yukon underscores another Cordilleran paleomagnetism-geology conundrum: Canadian Journal of Earth Sciences, 40, 1321-1334.
Tardy, M., 1980, Contribution a l'etude geologique de la Sierra Madre Oriental du Mexique: Paris, Université Pierre et Marie Curie, Doctoral thesis, 445 p.
Terrazas-Calderón, G. D., 2002, Cartografía, petrografía y geoquímica del intrusivo Cerro Mercado, Cinturón Candela-Monclova, Coahuila, México: Linares, Nuevo León, Universidad Autónoma de Nuevo León, Facultad de Ciencias de la Tierra, Tesis de Licenciatura, 102 p.
Tovar-Cortés, J.A., 2002, Geología y geoquímica del intrusivo Cerro Marcelinos, porción occidental del Cinturón Candela Monclova, Provincia Alcalina Oriental Mexicana: Linares, Nuevo León, Universidad Autónoma de Nuevo León, Facultad de Ciencias de la Tierra, Tesis de Licenciatura, 139 p.
Urrutia-Fucugauchi, J., 1981, Paleomagnetic evidence for tectonic rotation in northern Mexico and the continuity of the Cordilleran orogenic belt between Nevada and Chihuahua: Geology, 9, 178-183.
Valdez-Reyes, M.A., 2002, Petrografía y geoquímica del intrusivo Cerro Providencia, margen este del Cinturón Candela-Monclova, Provincia Alcalina Oriental Mexicana: Linares, Nuevo León, Universidad Autónoma de Nuevo León, Facultad de Ciencias de la Tierra, Tesis de Licenciatura, 109 p.
Vega-Vera, F.J., Perrilliat, M.C., 1989, La presencia del Eoceno marino en la cuenca de la Popa (Grupo Difunta), Nuevo León: orogenia post-Ypresiana: Universidad Nacional Autónoma de México, Revista del Instituto de Geología, 8, 67-70.
Ye, H., 1997, The arcuate Sierra Madre Oriental orogenic belt, NE Mexico: Tectonic infilling of a recess along the southwestern North America continental margin, *in* Soegaard, K., Giles, K., Vega, F., Lawton, T. (eds.), Structure, Stratigraphy and Paleontology of Late Cretaceous-Early Tertiary Parras-La Popa Foreland Basin near Monterrey, Northeast Mexico: American Association of Petroleum Geologists, Field Trip # 10, 85-115.
York, D., 1969, Least squares fitting of a straight line with correlated errors: Earth and Planetary Science Letters, 5, 320-324.
Zijderveld, J.D.A., 1967, A.C. demagnetization of rocks. Analysis Results, *in* Collins, D.W., Creer, K.M., Runcorn, S.K. (eds.), Methods in Paleomagnetism: Amsterdam, Elsevier, 251-286.

Manuscript received: May 11, 2007
Corrected manuscript received: February 12, 2008
Manuscript accepted: February 25, 2008